Published in final edited form as:
Vet Pathol. 2009 September ; 46(5): 1003–1014. doi:10.1354/vp.08-VP-0254-N-FL.

Expression of Tumor Invasion Factors Determines Systemic Engraftment and Induction of Humoral Hypercalcemia in a Mouse Model of Adult T-cell Leukemia

C. Parrula, **B. Zimmerman**, **P. Nadella**, **S. Shu**, **T. Rosol**, **S. Fernandez**, **M. Lairmore**, and **S. Niewiesk**

Department of Veterinary Biosciences, College of Veterinary Medicine (CP, BZ, PN, SS, TR, ML, SN), Division of Biostatistics, College of Public Health (SF), Comprehensive Cancer Center (TR, ML, SN), and Center for Retrovirus Research (TR, SF, ML, SN), Ohio State University, Columbus, OH

Abstract

Infection with human T-cell leukemia virus type 1 (HTLV-1) leads sometimes to the development of adult T-cell lymphoma/leukemia (ATL), which is invariably fatal and often associated with humoral hypercalcemia of malignancy. The transformation of infected CD4 T cells and the pathogenesis of leukemia have been studied with great limitation in tissue culture and patients. To better understand the pathogenesis and perform preclinical drug studies, animal models of ATL are urgently needed. In mice, inoculation of HTLV-1 cell lines mostly leads to development of localized lymphomas. To develop an ATL animal model with leukemic spread of ATL cells, mouse strains with different well-defined immune deficiencies were inoculated intraperitoneally with different HTLV-1–infected cell lines (ACH.2, C8166, MT-2, MET-1). Inoculation of MET-1 cells into NOD/SCID mice provided the best model system for slowly developing T-cell leukemia with multiple organ involvement. In leukemic mice, an increase in serum calcium levels correlated with expression of receptor activator of nuclear factor kappa-light-chain-enhancer of activated B cells ligand on leukemic cells and secretion of parathyroid hormone–related protein and interleukin-6. In contrast to the other cell lines that did not spread systemically, MET-1 expressed both the adhesion molecules CD11a (LFA-1α) and CD49d (VLA-4α) and produced or induced expression of matrix metalloproteinases 1, 2, 3, and 9, thus underlining the importance of these molecules in the spread of adult T-cell leukemia cells. The MET-1/NOD/SCID model will be useful for developing interventions against invasion and spread of leukemic cells and subsequent humoral hypercalcemia of malignancy.

Keywords

HTLV-1; matrix metalloproteinases; mouse model; systemic spread

Introduction

Worldwide 16 to 20 million people are infected with human T-cell leukemia virus type 1 (HTLV-1), and 1% to 5% of the infected individuals develop adult T-cell leukemia (ATL) during their lifetime13 due to transformation of their CD4 T cells. So far there is no successful therapeutic intervention for ATL.12 After chemotherapy and temporary remission of disease,

Request reprints from Dr. Stefan Niewiesk, College of Veterinary Medicine, Department of Veterinary Biosciences, Ohio State University, 1925 Coffey Road, Columbus, OH 43210 (USA). niewiesk.1@osu.edu..

tumor cells become invariably refractory to treatment and patients die within 9 to 24 months.36 Leukemic cells in ATL patients are very invasive, and the degree of organ infiltration affects disease profile and prognosis.3 A number of factors determining the spread of ATL cells have been defined based on studies of ATL cells from patients and in vitro studies. ATL cells are able to adhere to endothelial cells through high expression of CD11a (LFA-1α) and CD49d (VLA-4α).[38] Subsequently, the subendothelial basement membrane is thought to be degraded through the expression of matrix metalloproteinases (MMPs) 2 and 9 which lead to the retraction of endothelial cells and subsequent extravasation of neoplastic lymphocytes.2 The spread of tumor cells and high tumor burden releases factors that lead to the development of humoral hypercalcemia of malignancy9¯11،16،25 in most of the ATL patients. This disease condition is characterized by increased osteoclast activity with demineralization of bones and increased calcium levels in blood. It is thought that overexpression of receptor activator of nuclear factor κB ligand (RANKL) by ATL cells stimulates differentiation of hematopoietic precursors into osteoclasts.27 Parathyroid hormone–related protein (PTHrP), macrophage inflammatory protein 1-alpha (MIP-1α), tumor necrosis factor-alpha (TNF-α), interleukin-1 (IL-1), and IL-6 are also thought to be important in enhancing migration and differentiation of osteoclast progenitors into mature osteoclasts by stimulating production of RANKL by osteoblasts and stromal cells.34 Interestingly enough, the activation of most of the above-named molecules has been shown to be due to nuclear factor kappa-light-chain-enhancer of activated B cells activation through Tax expression (at least in tissue culture), indicating a role for Tax in metastasis and hypercalcemia.22،23

Although these putative steps in the pathogenesis of disease are supported by evidence derived from tissue culture experiments and clinical observations in patients, animal models are required to verify these concepts.[19] For this reason, a number of xenograft mouse models have been established.[7,20,28,32,37] The drawback for most of these models is the fact that inoculated HTLV-1–infected permanent cell lines usually do not spread systemically but grow either subcutaneously after subcutaneous inoculation or in the abdominal cavity after intraperitoneal injection.[7,20,28,32,37] In this study, we tested different HTLV-1–infected cell lines for their ability to induce multicentric engraftment in 3 different mouse lines and used the resulting MET-1/NOD/SCID mouse model to address hypercalcemia of malignancy and the role of adhesion molecules and matrix MMPs for tumor spread.

Methods

Animals

Female immunodeficient NOD/SCID (NOD.CB17-Prkdc^{scid}/J), NOD/SCID$^{\beta 2m-/-}$ (NOD.Cg-Prkdc^{scid} B2m^{tm1Unc}/J) (The Jackson Laboratory, Bar Harbor, ME), and NOD/SCID$^{Il2rg\gamma\ -/-}$ with a deleted (NOD.Cg-Prkdc^{scid} Il2rg^{tm1Wjl}/SzJ) (The Jackson Laboratory) or truncated IL-2-Rγ gene (NODShi.Cg-Prkdc^{scidIl2rgtm1Sug}/Jic) (Central Institute for Experimental Animals, Kawasaki, Japan) mice (Table 1), were inoculated with 10^7 tumor cells intraperitoneally. Animals were monitored and weighed regularly after inoculation. Mice were euthanatized using CO_2 inhalation as soon as they developed signs of morbidity. All animal experiments were approved by the Institutional Animal Care and Use Committee of Ohio State University.

Cell lines

The HTLV-I–infected cell lines MT-2[40] and C8166-45[35] were maintained in advanced RPMI 1640 medium supplemented with 10% fetal bovine serum. For the ACH.2 cell line,[6] 10 IU/mL rIL-2 was added. MET-1 cells were derived from a patient with ATL[31] and expanded in NOD/SCID mice.

Flow cytometry analysis

For detection of proteins expressed at the cell surface, antibodies specific for RANKL (clone 12A668, Calbiochem), CD11a (LFA-1; clone G43-25B), CD49d (9F10), CD147 (extracellular matrix metalloproteinases [EMMPRIN], clone HIM6), and isotype controls (clones G155-178 and MOPC-21; all from BD Biosciences Pharmingen, San Diego, CA) were used.

Total calcium measurement in serum

Total calcium was measured from serum by a colorimetric assay based on the reaction of Ca^{2+} with arsenazo III dye and analyzed in a Vitros DT60 Chemistry Analyzer (Ortho-Clinical Diagnostics, Rochester, NY). Statistical analysis was performed using the Kruskal-Wallis test.

Measurement of PTHrP

PTHrP was measured from plasma by the DSL-8100 ACTIVE PTHrP coated–tube immunoradiometric assay kit according to the instructions of the manufacturer (Diagnostic Systems Laboratories, Webster, TX).

Histopathology and immunohistochemistry

Tissues were fixed, paraffin embedded, and stained with HE or antibody specific for Ki-67 (clone Ki-S5) (Dako, Glostrup, Denmark) or MMP1, 2, 3, or 9 according to standard procedures using Dako's biotin blocking kit, Dako's target retrieval solution, and biotinylated secondary antibodies (goat-anti-rabbit antiserum or rabbit-anti-goat antiserum) (Vector Laboratories, Burlingame, CA).

Western blot

MET-1, MT-2, C8166-45 cells were lysed for 30 minutes on ice in 20 mM Tris-HCl (pH 7.50), 150 mM NaCl, 1% Triton, 1 mM Na_2EDTA, 1 μg/mL leupeptin, 1 mM phenylmethysulfonyl fluoride, 1 mM Na_3Vo_4, 1 mM EGTA, 2.5 mM sodium pyrophosphate, and 1 mM beta-glycerophosphate. Lysates and controls (Chemicon International, Temecula, CA) (30 μg/lane) were separated by sodium dodecyl sulfate polyacrylamide gel electrophoresis through a Nupage Novex 10% Bis-Tris precast gel, followed by transfer to nitrocellulose membranes (Bio-Rad, Hercules, CA). The membranes were blocked and incubated with antibody specific for MMPs and a glyceraldehyde 3-phosphate dehydrogenase control antibody (clone 1D4) (Nventa Biopharmaceuticals Corporation, Montreal, Quebec, Canada) and the respective secondary antibody. Blots were developed with the ECLplus detection system (GE Healthcare, Waukesha, WI).

Cytokine array

Sera from 2 groups of NOD/SCID mice inoculated with MET-1 cells (1×10^7 cells/mouse) were pooled and analyzed for the presence of human cytokines with an array membrane (TranSignal Human Cytokine Antibody Array 1.0) (Panomics, Fremont, CA). Pooled sera from naïve NOD/SCID mice were used as controls. Membranes were treated according to the manufacturer's protocol, incubated with ECLplus (GE Healthcare), and scanned with the Typhoon 9410, GE Healthcare. The images acquired were analyzed for quantitative data using ImageQuant software (GE Healthcare).

Polymerase chain reactions

Total RNA was extracted using Trizol Reagent (Invitrogen, Carlsbad, CA) and was treated with the TURBO DNA*free* Kit (Ambion, Austin, TX). The cDNA was amplified with primers for MMP9 (5′-CGCAGACATCGTCATCCAGT-3′ and 5′-GGATTGGCCTTGGAAGATGA-3′) and MIP-1α 5′-GCAACCAGTTCTCTGCATCA-3′

and 5′-TTTCTGGACCCACTCCTCAC-3′). The tax primers span the splice site in HTLV-1 and are cDNA specific.14 IL-1β and TNF-α primers were used as published.17,39 Quantitative real-time polymerase chain reaction (RT-PCR) of PTHrP (corresponding to 0.1 μg of RNA/sample) was performed using SYBR Green PCR kit (Qiagen, Hilden, Germany) according to the manufacturer's protocol in a LightCycler apparatus (Roche Diagnostics, Indianapolis, IN) as described previously.33 Briefly, primers for the PTHrP common region (5′-GTCTCAGCCGCCGCCTCAA-3′ and 5′-GGAAGAATCGTCGCCGTAAA-3′) were used to amplify cDNA and plasmid standard. For normalization, β2-microglobulin cDNA was used.

Results

Inoculation of 3 different immunodeficient mouse strains with ATL cells

To establish an animal model with systemic spread of ATL, cells of 4 different HTLV-1–infected cell lines (Table 2) were inoculated into 3 different mouse strains based on the NOD/SCID background (Table 1). All cell lines chosen were HTLV-1–infected human CD4-positive T-cell lines but differed in their expression levels of HTLV-1 viral proteins. ACH-2 cells were derived from peripheral blood lymphocytes after immortalization with a molecular clone of HTLV-1. These cells express all HTLV-1 proteins and depend on IL-2 for growth in tissue culture.[6] Although these cells do not grow as robustly as other HTLV-1–transformed cell lines, the possibility of transforming cells with a molecular clone that can be modified is attractive for further pathogenesis or infectivity investigations. C8166-45 and MT-2 cells were derived from coculture of peripheral blood lymphocytes with ATL cells from a patient. C8166-45 cells contain 2 copies of the HTLV-1 genome but express only the Tax protein, because other genes are inactivated by deletions or stop mutations, respectively.4 MT-2 cells carry 4 to 6 HTLV-1 genomes and express all HTLV-1 proteins.18,40 MET-1 cells are derived from an ATL patient and can be passaged only in mice.[31] Using MET-1 cells, we demonstrated the expression of HTLV-1 envelope protein by flow cytometry and expression of tax by RT-PCR, although expression could only be detected when 500 ng of total RNA per RT-PCR reaction was used (data not shown).

Animals were inoculated intraperitoneally with 1×10^7 cells and euthanized after displaying severe clinical symptoms or at the end of the experiment. ACH-2 and C8166-45 cells did not engraft. Both cell lines express Tax protein, which indicates that Tax alone is not sufficient for engraftment of cells.

MT-2 cells formed small tumor nodules in the abdominal cavity in 2 of 5 NOD/SCID and NOD/SCID$^{\beta 2m-/-}$ mice. In NOG mice, however, MT-2 cells engrafted within 3 to 4 weeks by forming tumors in the peritoneal cavity of all animals and in the thoracic cavity of 2 of 5 animals. MET-1 cells engrafted in NOD/SCID mice within 12 to 14 weeks and in NOD/SCID$^{\beta 2m-/-}$ mice within 9 to 12 weeks (Table 2). The reported reduction in natural killer–cell activity correlated with success of and time necessary for engraftment of tumor cells. It has been proposed that the Tax protein of HTLV-1 might be a target for natural killer cells.[20] However, in spite of Tax expression, MT-2 and MET-1 cells are able to engraft (although to different degrees) in NOD/SCID mice.

Pattern of spread and tumor invasion of MT-2 and MET-1 cells

Most tumor cell lines (whether HTLV-1 transformed or not) grow in immune-deficient mice after intraperitoneal inoculation in the peritoneal cavity. The engraftment pattern after intraperitoneal inoculation of MT-2 cells, therefore, is typical for most of the engrafting permanent cell lines used in mice, which are rarely truly leukemic with systemic spread of tumor cells. In the blood smears of animals inoculated with MT-2 cells, no abnormal cells were found (Fig. 1). MT-2 cells remained mostly in the peritoneal cavity, and only in 2 of 5 animals

was involvement of the thoracic cavity observed. Solid tumors displayed a capsular pattern and were attached to organs, most commonly the pancreas (Figs. 2, 3) and liver, but also the ovary, uterus, kidney, and stomach. (The human origin of these tumor cells was confirmed by Ki67 staining (Fig. 3b). Tumor formation was usually accompanied by neutrophilic infiltrates in affected organs (Fig. 2), and sometimes tumors were necrotic.

After engraftment, MET-1 cells could be detected in blood smears (Fig. 4) at the time of euthanasia, indicating systemic spread of leukemic cells. Tumor cells invaded organs perivascularly and were found in organs of the peritoneal (pancreas, liver, kidney, uterus, stomach, intestine, peritoneum, urinary bladder) and thoracic cavities (adrenal, heart [Fig. 5], lung [Fig. 6]), as well as brain and skin at the site of injection. The human origin of the cells was confirmed by staining for the human Ki67 antigen (Fig. 3b). This MET-1/NOD/SCID model recapitulates the tumor invasion pattern seen in ATL patients.

Increased calcium levels in serum of mice inoculated with MET-1 cells

Because the spread of MET-1 cells in NOD/SCID mice was similar to that detected in human patients, we refined the model by defining hypercalcemia in these animals. A large proportion of ATL patients develop humoral hypercalcemia of malignancy. This condition is characterized by increased calcium and PTHrP levels in serum and increased osteolysis (bone resorption).[29] In control mice, calcium levels were 9.7 ± 1.2 mg/dL for NOD/SCID mice and 9.7 ± 0.7 mg/dL for NOD/SCID$^{\beta 2m-/-}$. The calcium levels in NOD/SCID and NOD/SCID$^{\beta 2m-/-}$ mice inoculated with MET-1 cells were significantly higher ($P < .05$, Kruskal-Wallis test) than those of control animals (13.8 ± 3.6 mg/dL for NOD/SCID mice and 17.1 ± 4.8 mg/dL for NOD/SCID$^{\beta 2m-/-}$) (Fig. 7). PTHrP protein was detected in the plasma of all mice inoculated with MET-1 (19 ± 21.8 pmol/L in NOD/SCID mice and 16.8 ± 21.7 pmol/L in NOD/SCID$^{\beta 2m-/-}$), but no PTHrP was detected in serum of control mice (Fig. 8). In MET-1 cells, PTHrP mRNA was quantified as 20 to 25 copies per 10^4 copies of glyceraldehyde 3-phosphate dehydrogenase. The expression of PTHrP mRNA by MET-1 cells correlated with PTHrP protein in serum of mice (data not shown). It is thought that PTHrP plays an important role in stimulating osteoclasts, resulting in increased bone resorption. However, PTHrP cannot induce the differentiation of hematopoietic precursor cells to osteoclasts directly, and RANKL and a number of cytokines and chemokines are likely to be involved in the process. In support of this model, expression of RANKL was shown on MET-1 cells ex vivo, with 33% of the cells being positive by flow cytometry after stain with an anti-RANKL antibody (Fig. 9). The expression of a variety of chemokines and cytokines in sera from mice inoculated with MET-1 cells was measured with a human cytokine array. IL-6 was found in the sera (Fig. 10), but no other factors (IL-1β, TNF-α, or MIP-1α) involved in humoral hypercalcemia were detected by the cytokine array. However, a confirmatory PCR assay revealed IL-1β mRNA, but no mRNA expression of TNF-α or MIP-1α could be detected in ex vivo–derived MET-1 cells.

Comparison of tumor invasion factors among MT-2, MET-1, and C8166-45 cells

The difference seen in the engraftment in NOD/SCID and NOD/SCID$^{\beta 2m-/-}$ mice may be explained by differences in natural killer–cell activity. However, in NOG mice, which have virtually no functional immune system, the difference seen between MT-2 cells and C8166-45 cells must be due to expression of tumor invasion factors by these cells. ATL cells have been found to express increased levels of certain adhesion molecules (CD11a, CD49d), MMPs, and EMMPRIN, which have been implicated in tumor invasion. To investigate a correlation between tumor invasion factors and the engraftment of the cell lines used in this study, we compared the expression of CD11a; CD49d; MMP1, 2, 3, and 9; and EMMPRIN (CD147) between MET-1, MT-2, and C8166-45 cells. All cell lines expressed EMMPRIN. MET-1 cells expressed both CD11a and CD49d (Fig. 11), whereas MT-2 expressed only CD49d; C8166-45 expressed only low amounts of CD11a.

To compare the ability of tumor cells to invade tissues, the cells were tested for the expression of MMP1, 2, 3, and 9. MET-1 cells expressed MMP1 and MMP3 but no MMP2 and 9 by Western blot (Fig. 12 and data not shown, respectively). The absence of MMP9 also was confirmed by RT-PCR (data not shown), because the expression of MMP9 in ATL cells was reported previously.[24] MT-2 and C8166-45 cells weakly expressed MMP1 but no MMP2, MMP3, or MMP9 by Western blot. All MMPs can be expressed by either the tumor cell or by the fibroblasts surrounding tumor cells in the stroma. In other tumor systems, MMP2 and 9 often are expressed by surrounding fibroblasts, whereas MMP1 and 3 are typically are expressed by tumor cells.8 Our results are consistent with results obtained from other tumors. To test the expression levels and localizations of MMPs in vivo, immunohistochemistry was performed on tumor tissues. In tumors induced by MET-1, expression of MMP1, MMP2, and MMP3 was found in situ (Fig. 13). In addition, weak expression of MMP9 was detected. In contrast, in tumors formed by MT-2 cells, only MMP1 was expressed weakly by a small percentage of tumor cells, whereas MMP2, 3, and 9 were expressed in only a few single tumor cells in vivo (Fig. 14).

Discussion

An interesting finding in the MET-1/NOD/SCID model was the correlation between PTHrP expression and increased calcium levels in the blood. Although the rise in serum PTHrP makes biologic sense and was observed in another mouse model,[32] this is not consistently found in ATL patients.[10,11,16] Of all the cytokines and chemokines thought to be important in activating osteoclast activity,[29,34] only high levels of IL-6 were found to be expressed in serum of mice with MET-1 tumor burden, and low levels of IL-1β mRNA were detected by PCR. This is of interest because a nucleotide variant of the IL-6–promotor region was found to be associated with low bone density in humans,[30] and certain haplo-types of IL-6 are associated with increased risk of HTLV-1 infection in children.[5] Thus, IL-6 might be a link between infection and development of humoral hypercalcemia of malignancy. In addition to IL-6, IL-4 and IL-12 were found in serum from mice inoculated with MET-1. Both IL-12[1,15] and IL-4[21] have been described as inhibitors of osteoclast activity, and their expression suggests a regulatory role for these cytokines in osteoclast activation in vivo.

In this study, the differences between the widespread engraftment of MET-1 cells, the poor engraftment of MT-2, and the lack of engraftment of C8166-45 cells correlate with the expression of integrins and MMPs. These molecules are thought to be important in ATL invasion based on observations in patient samples.2 A first step in the invasion of tissue by ATL tumor cells is the adherence to vascular endothelial cells through CD11a and CD49d,[38] similar to activated T cells. The fact that only MET-1 cells express both CD11a and CD49d, whereas MT-2 and C8166-45 express only one or the other, supports this concept. Another group of molecules important for tumor invasion consists of the EMMPRIN (CD147) and MMPs. It has been reported that ATL cells express EMMPRIN and MMP9[24] ex vivo, and MMP2 expression has been demonstrated in skin biopsies from ATL patients,26 suggesting the importance of MMPs in the development of ATL. In this study, all cell lines expressed EMMPRIN, indicating that EMMPRIN expression is not sufficient for engraftment. In vitro, both MMP1 and MMP3 were expressed by MET-1, whereas neither MMP2 nor MMP9 was expressed. In vivo, MET-1 expressed all the MMPs tested, although MMP9 was expressed weakly. Although it has been reported that MMP9 is expressed ex vivo by ATL cells,24 the data for MET-1 are in line with other tumor models in which MMP1 and 3 were expressed by tumor cells and MMP2 and 9 expression was induced in vivo.8 Our data demonstrate that the MET-1/NOD/SCID model is an excellent model to define tumor invasion factors and, for example, to test the efficacy of MMP inhibitors on the spread of ATL cells. It should be noted as well that the involvement of other MMPs needs to be addressed in this model. For example,

it has been shown that MMP14 is a necessary requisite for MMP2 expression.[8] Therefore, the intricate interactions required for invasion of leukemic cells need to be further investigated.

Acknowledgments

The following reagents were obtained through the AIDS Research and Reference Reagent Program, Division of AIDS, NIAID, NIH: MT-2 from Dr. Douglas Richman and C8866-45 from Dr. Robert Gallo. MET-1 cells were obtained from Dr. Thomas Waldman at NCI, NIH.

References

1. Amcheslavsky A, Bar-Shavit Z. Interleukin (IL)-12 mediates the anti-osteoclastogenic activity of CpG-oligodeoxynucleotides. J Cell Physiol 2006;207:244–250. [PubMed: 16402377]
2. Bazarbachi A, Abou Merhi R, Gessain A, Talhouk R, El-Khoury H, Nasr R, Gout O, Sulahian R, Homaidan F, de The H, Hermine O, El-Sabban ME. Human T-cell lymphotropic virus type I-infected cells extravasate through the endothelial barrier by a local angiogenesis-like mechanism. Cancer Res 2004;64:2039–2046. [PubMed: 15026341]
3. Bazarbachi A, Ghez D, Lepelletier Y, Nasr R, de The H, El-Sabban ME, Hermine O. New therapeutic approaches for adult T-cell leukaemia. Lancet Oncol 2004;5:664–672. [PubMed: 15522654]
4. Bhat NK, Adachi Y, Samuel KP, Derse D. HTLV-1 gene expression by defective proviruses in an infected T-cell line. Virology 1993;196:15–24. [PubMed: 8356792]
5. Brown EE, Brown BJ, Yeager M, Welch R, Cranston B, Hanchard B, Hisada M. Haplotypes of IL6 and IL10 and susceptibility to human T lymphotropic virus type I infection among children. J Infect Dis 2006;194:1565–1569. [PubMed: 17083041]
6. Collins ND, D'Souza C, Albrecht B, Robek MD, Ratner L, Ding W, Green PL, Lairmore MD. Proliferation response to interleukin-2 and Jak/Stat activation of T cells immortalized by human T-cell lymphotropic virus type 1 is independent of open reading frame I expression. J Virol 1999;73:9642–9649. [PubMed: 10516077]
7. Dewan MZ, Terashima K, Taruishi M, Hasegawa H, Ito M, Tanaka Y, Mori N, Sata T, Koyanagi Y, Maeda M, Kubuki Y, Okayama A, Fujii M, Yamamoto N. Rapid tumor formation of human T-cell leukemia virus type 1-infected cell lines in novel NOD-SCID/gammac(null) mice: suppression by an inhibitor against NF-kappaB. J Virol 2003;77:5286–5294. [PubMed: 12692230]
8. Egeblad M, Werb Z. New functions for the matrix metalloproteinases in cancer progression. Nat Rev Cancer 2002;3:161–174. [PubMed: 11990853]
9. Fukumoto S, Matsumoto T, Watanabe T, Takahashi H, Miyoshi I, Ogata E. Secretion of parathyroid hormone-like activity from human T-cell lymphotropic virus type I-infected lymphocytes. Cancer Res 1989;49:3849–3852. [PubMed: 2544261]
10. Grossman B, Schechter GP, Horton JE, Pierce L, Jaffe E, Wahl L. Hypercalcemia associated with T-cell lymphoma-leukemia. Am J Clin Pathol 1981;75:149–155. [PubMed: 6970519]
11. Haratake J, Ishii N, Horie A, Matsumoto M, Oda S, Satoh K. Adult T-cell leukemia complicated by hypercalcemia: report of three autopsy cases with special reference to the etiologic factor of hypercalcemia. Acta Pathol Jpn 1985;35:437–448. [PubMed: 3875211]
12. Ishikawa T. Current status of therapeutic approaches to adult T-cell leukemia. Int J Hematol 2003;78:304–311. [PubMed: 14686487]
13. Kannagi M, Ohashi T, Harashima N, Hanabuchi S, Hasegawa A. Immunological risks of adult T-cell leukemia at primary HTLV-I infection. Trends Microbiol 2004;12:346–352. [PubMed: 15223062]
14. Kinoshita T, Shimoyama M, Tobinai K, Ito M, Ito S, Ikeda S, Tajima K, Shimotohno K, Sugimura T. Detection of mRNA for the tax1/rex1 gene of human T-cell leukemia virus type I in fresh peripheral blood mononuclear cells of adult T-cell leukemia patients and viral carriers by using the polymerase chain reaction. Proc Natl Acad Sci USA 1989;86:5620–5624. [PubMed: 2787512]
15. Kitaura H, Nagata N, Fujimura Y, Hotokezaka H, Yoshida N, Nakayama K. Effect of IL-12 on TNF-alpha-mediated osteoclast formation in bone marrow cells: apoptosis mediated by Fas/Fas ligand interaction. J Immunol 2002;169:4732–4738. [PubMed: 12391181]

16. Kiyokawa T, Yamaguchi K, Takeya M, Takahashi K, Watanabe T, Matsumoto T, Lee SY, Takatsuki K. Hypercalcemia and osteoclast proliferation in adult T-cell leukemia. Cancer 1987;59:1187–1191. [PubMed: 2880656]

17. Klein SC, van Wichen DF, Golverdingen JG, Jacobse KC, Broekhuizen R, de Weger RA. An improved, sensitive, non-radioactive in situ hybridization method for the detection of cytokine mRNAs. Apmis 1995;103:345–353. [PubMed: 7654359]

18. Kobayashi N, Konishi H, Sabe H, Shigesada K, Noma T, Honjo T, Hatanaka M. Genomic structure of HTLV (human T-cell leukemia virus): detection of defective genome and its amplification in MT-2 cells. EMBO J 1984;3:1339–1343. [PubMed: 6086318]

19. Lairmore MD, Silverman L, Ratner L. Animal models for human T-lymphotropic virus type 1 (HTLV-1) infection and transformation. Oncogene 2005;24:6005–6015. [PubMed: 16155607]

20. Liu Y, Dole K, Stanley JR, Richard V, Rosol TJ, Ratner L, Lairmore M, Feuer G. Engraftment and tumorigenesis of HTLV-1 transformed T cell lines in SCID/bg and NOD/SCID mice. Leuk Res 2002;26:561–567. [PubMed: 12007504]

21. Lubberts E, Joosten LA, Chabaud M, van Den Bersselaar L, Oppers B, Coenen-De Roo CJ, Richards CD, Miossec P, van Den Berg WB. IL-4 gene therapy for collagen arthritis suppresses synovial IL-17 and osteoprotegerin ligand and prevents bone erosion. J Clin Invest 2000;105:1697–1710. [PubMed: 10862785]

22. Matsuoka M. Human T-cell leukemia virus type I and adult T-cell leukemia. Oncogene 2003;22:5131–5140. [PubMed: 12910250]

23. Matsuoka M, Jeang KT. Human T-cell leukaemia virus type 1 (HTLV-1) infectivity and cellular transformation. Nat Rev Cancer 2007;7:270–280. [PubMed: 17384582]

24. Mori N, Sato H, Hayashibara T, Senba M, Hayashi T, Yamada Y, Kamihira S, Ikeda S, Yamasaki Y, Morikawa S, Tomonaga M, Geleziunas R, Yamamoto N. Human T-cell leukemia virus type I Tax transactivates the matrix metalloproteinase-9 gene: potential role in mediating adult T-cell leukemia invasiveness. Blood 2002;99:1341–1349. [PubMed: 11830485]

25. Motokura T, Fukumoto S, Matsumoto T, Takahashi S, Fujita A, Yamashita T, Igarashi T, Ogata E. Parathyroid hormone-related protein in adult T-cell leukemia-lymphoma. Ann Intern Med 1989;111:484–488. [PubMed: 2549824]

26. Nabeshima K, Suzumiya J, Nagano M, Ohshima K, Toole BP, Tamura K, Iwasaki H, Kikuchi M. Emmprin, a cell surface inducer of matrix metalloproteinases (MMPs), is expressed in T-cell lymphomas. J Pathol 2004;202:341–351. [PubMed: 14991900]

27. Nosaka K, Miyamoto T, Sakai T, Mitsuya H, Suda T, Matsuoka M. Mechanism of hypercalcemia in adult T-cell leukemia: overexpression of receptor activator of nuclear factor kappaB ligand on adult T-cell leukemia cells. Blood 2002;99:634–640. [PubMed: 11781248]

28. Ohsugi T, Yamaguchi K, Kumasaka T, Ishida T, Horie R, Watanabe T, Sakio N, Fujimoto T, Sakamoto N, Urano T. Rapid tumor death model for evaluation of new therapeutic agents for adult T-cell leukemia. Lab Invest 2004;84:263–266. [PubMed: 14688803]

29. Okada Y, Tsukada J, Nakano K, Tonai S, Mine S, Tanaka Y. Macrophage inflammatory protein-1alpha induces hypercalcemia in adult T-cell leukemia. J Bone Miner Res 2004;19:1105–1111. [PubMed: 15176993]

30. Ota N, Nakajima T, Nakazawa I, Suzuki T, Hosoi T, Orimo H, Inoue S, Shirai Y, Emi M. A nucleotide variant in the promoter region of the interleukin-6 gene associated with decreased bone mineral density. J Hum Genet 2001;46:267–272. [PubMed: 11355017]

31. Phillips KE, Herring B, Wilson LA, Rickford MS, Zhang M, Goldman CK, Tso JY, Waldmann TA. IL-2R alpha-directed monoclonal antibodies provide effective therapy in a murine model of adult T-cell leukemia by a mechanism other than blockade of IL-2/IL-2Ralpha interaction. Cancer Res 2000;60:6977–6984. [PubMed: 11156399]

32. Richard V, Lairmore MD, Green PL, Feuer G, Erbe RS, Albrecht B, D'Souza C, Keller ET, Dai J, Rosol TJ. Humoral hypercalcemia of malignancy: severe combined immunodeficient/beige mouse model of adult T-cell lymphoma independent of human T-cell lymphotropic virus type-1 tax expression. Am J Pathol 2001;158:2219–2229. [PubMed: 11395400]

33. Richard V, Luchin A, Brena RM, Plass C, Rosol TJ. Quantitative evaluation of alternative promoter usage and 39 splice variants for parathyroid hormone-related protein by real-time reverse transcription-PCR. Clin Chem 2003;49:1398–1402. [PubMed: 12881458]

34. Roodman GD. Regulation of osteoclast differentiation. Ann N Y Acad Sci 2006;1068:100–109. [PubMed: 16831910]

35. Salahuddin SZ, Markham PD, Wong-Staal F, Franchini G, Kalyanaraman VS, Gallo RC. Restricted expression of human T-cell leukemia–lymphoma virus (HTLV) in transformed human umbilical cord blood lymphocytes. Virology 1983;129:51–64. [PubMed: 6412453]

36. Shimoyama M. Diagnostic criteria and classification of clinical subtypes of adult T-cell leukemia-lymphoma: a report from the Lymphoma Study Group (1984–1987). Br J Haematol 1991;79:428–437. [PubMed: 1751370]

37. Takaori-Kondo A, Imada K, Yamamoto I, Kunitomi A, Numata Y, Sawada H, Uchiyama T. Parathyroid hormone-related protein-induced hypercalcemia in SCID mice engrafted with adult T-cell leukemia cells. Blood 1998;91:4747–4751. [PubMed: 9616173]

38. Tanaka Y, Mine S, Figdor CG, Wake A, Hirano H, Tsukada J, Aso M, Fujii K, Saito K, van Kooyk Y, Eto S. Constitutive chemokine production results in activation of leukocyte function-associated antigen-1 on adult T-cell leukemia cells. Blood 1998;91:3909–3919. [PubMed: 9573029]

39. Van Hoffen E, Van Wichen D, Stuij I, De Jonge N, Klopping C, Lahpor J, Van Den Tweel J, Gmelig-Meyling F, De Weger R. In situ expression of cytokines in human heart allografts. Am J Pathol 1996;149:1991–2003. [PubMed: 8952534]

40. Yamamoto N, Okada M, Koyanagi Y, Kannagi M, Hinuma Y. Transformation of human leukocytes by cocultivation with an adult T cell leukemia virus producer cell line. Science 1982;217:737–739. [PubMed: 6980467]

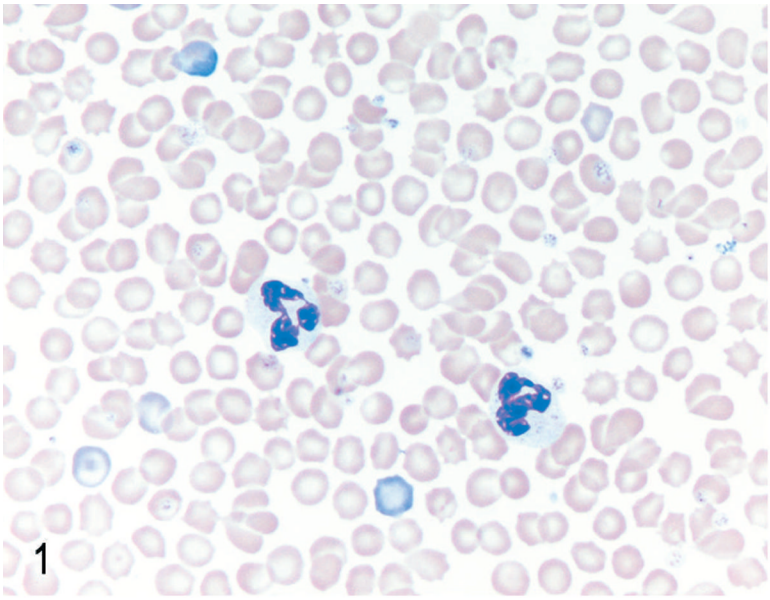

Fig. 1.
Blood. NOD/SCID$^{\beta 2m-/-}$ mouse inoculated with MT-2 cells. No abnormal cells were found in peripheral blood. Two neutrophils seen in the middle of field. Wright stain.

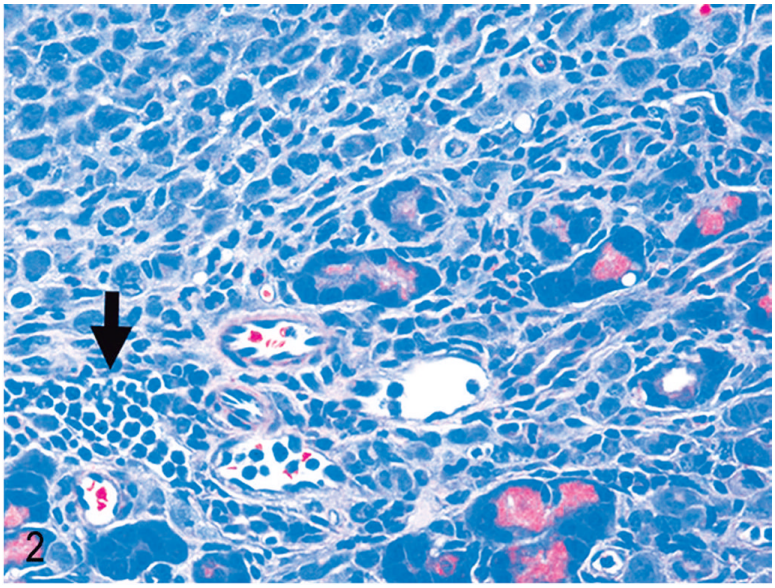

Fig. 2.
Pancreas. NOD/*SCID*$^{Il2rg\ -/-}$ mouse inoculated with MT-2 cells. Neutrophils (arrow) usually accompany MT-2 infiltration of tissues. HE.

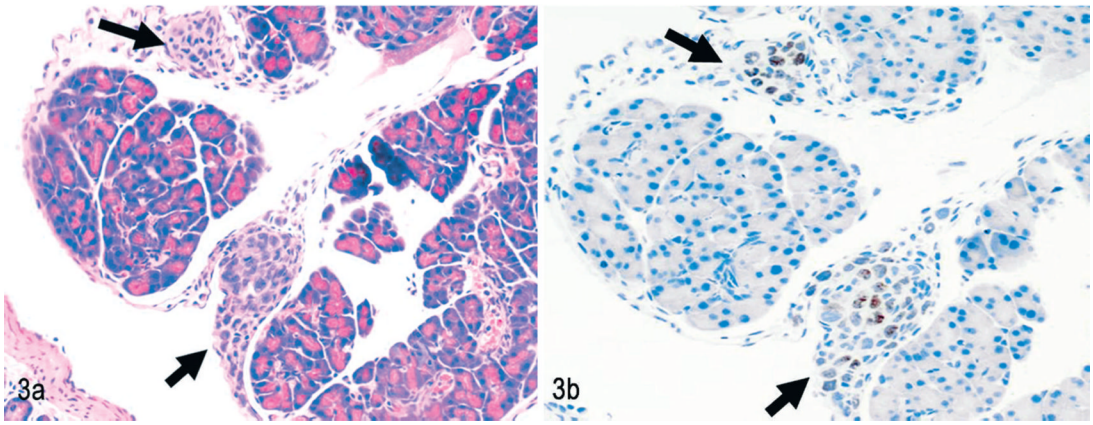

Fig. 3.
Pancreas. NOD/*SCID*$^{Il2rg\ -/-}$ mouse inoculated with MT-2 cells. Invasion is pericapsular. Black arrows indicate small aggregates of MT-2 cells attached to the capsule. **Fig. 3a.** HE. **Fig. 3b.** Immunolabeling with mAb anti-human Ki67 and hematoxylin counterstain.

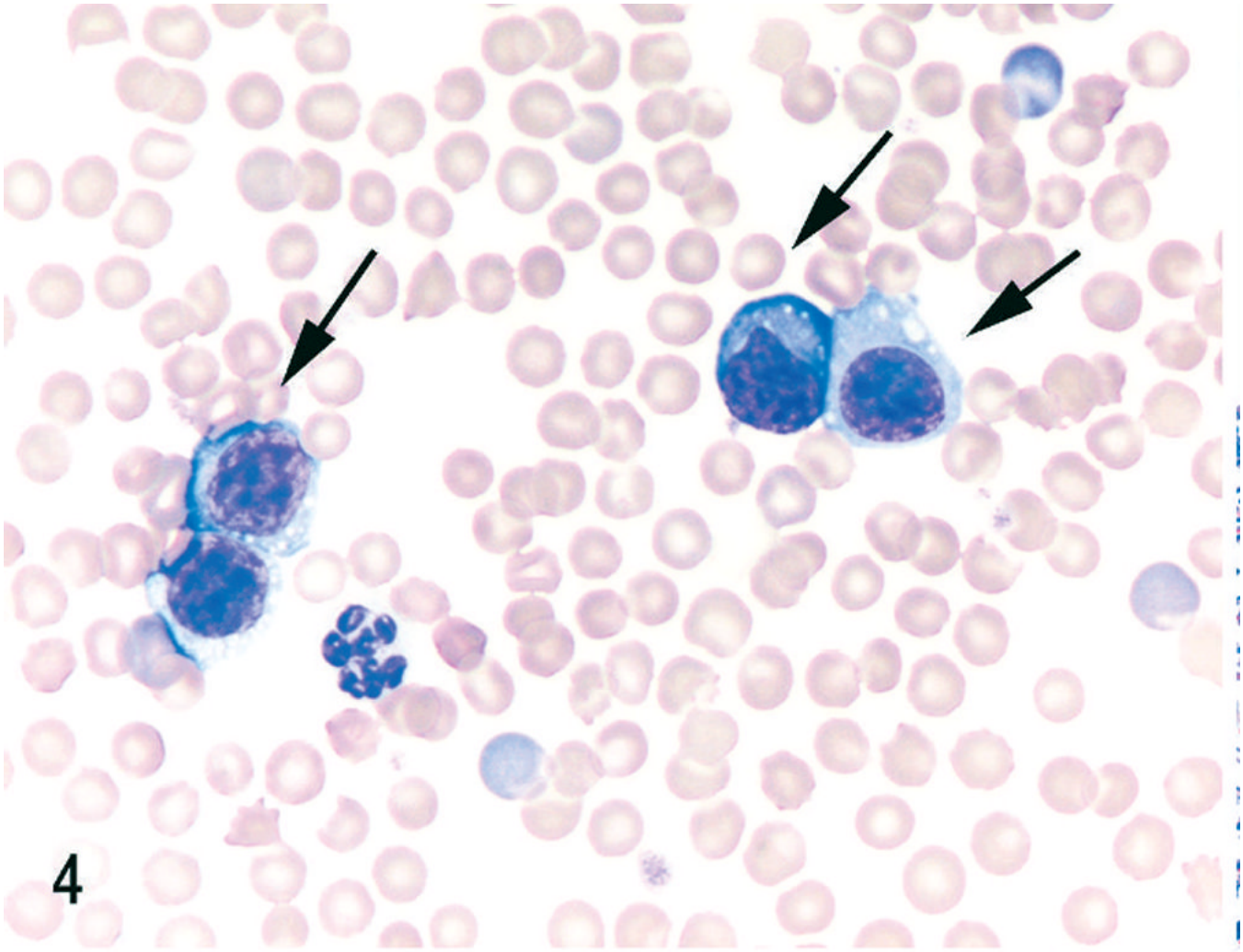

Fig. 4.
Blood. NOD/SCID$^{\beta 2m-/-}$ mouse inoculated with MET-1 cells. Large aberrant round cells (MET-1) with round to irregularly shaped nuclei and fine chromatin are present (arrows). Wright stain.

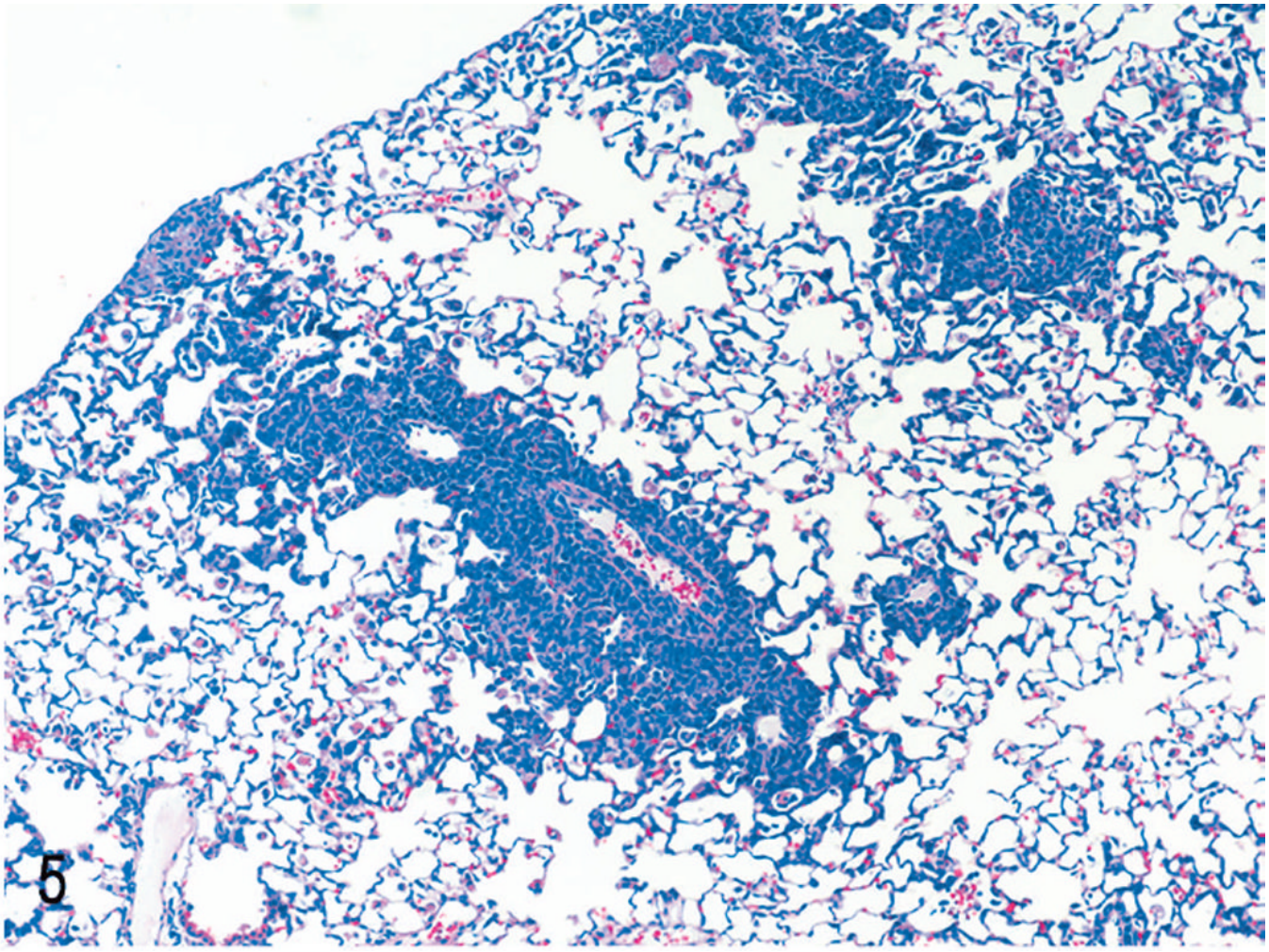

Fig. 5.
Lung. NOD/SCID$^{\beta 2m-/-}$ mouse inoculated with MET-1 cells. MET-1 cells have a perivascular pattern of invasion. HE.

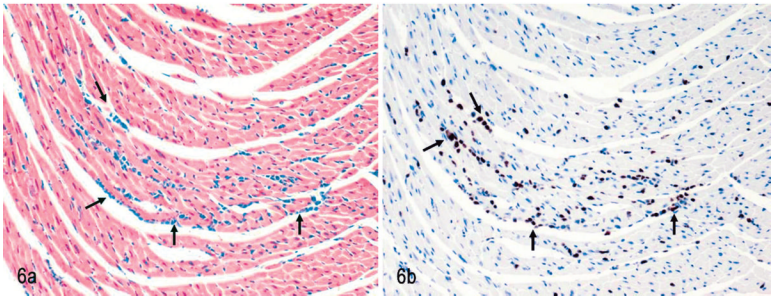

Fig. 6.

Heart. NOD/SCID$^{\beta 2m-/-}$ mouse inoculated with MET-1 cells. Tumor cells have infiltrated between cardiac muscle fibers arrows. **Fig. 6a.** HE. **Fig. 6b.** Tumor cells show positive nuclear staining with an antibody specific for human Ki67, confirming the human origin of cells. Immunolabeling with mAb anti-human Ki67 and hematoxylin counterstain.

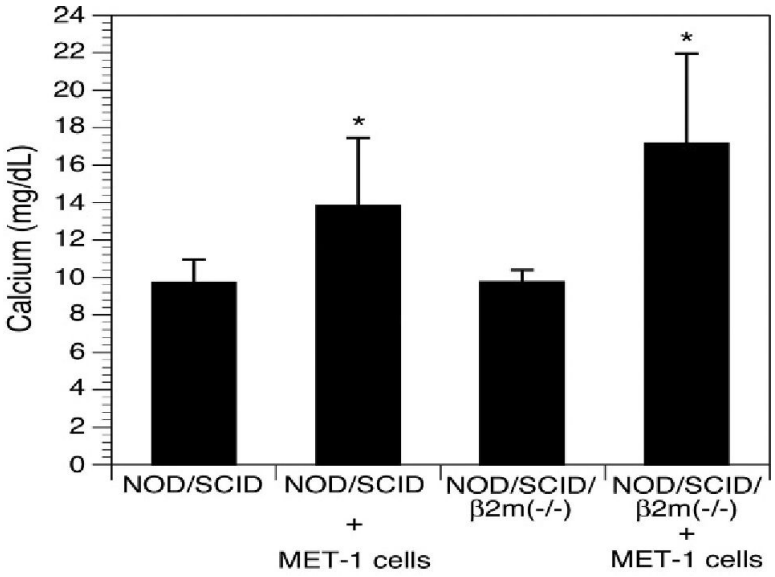

Fig. 7.

Calcium levels. Calcium levels were significantly increased in NOD/SCID (8 animals/group) and NOD/SCID$^{\beta 2m-/-}$ mice (5 animals/group) inoculated with MET-1 cells ($P < .05$, Kruskal-Wallis test) compared with naïve animals (5 animals/group).

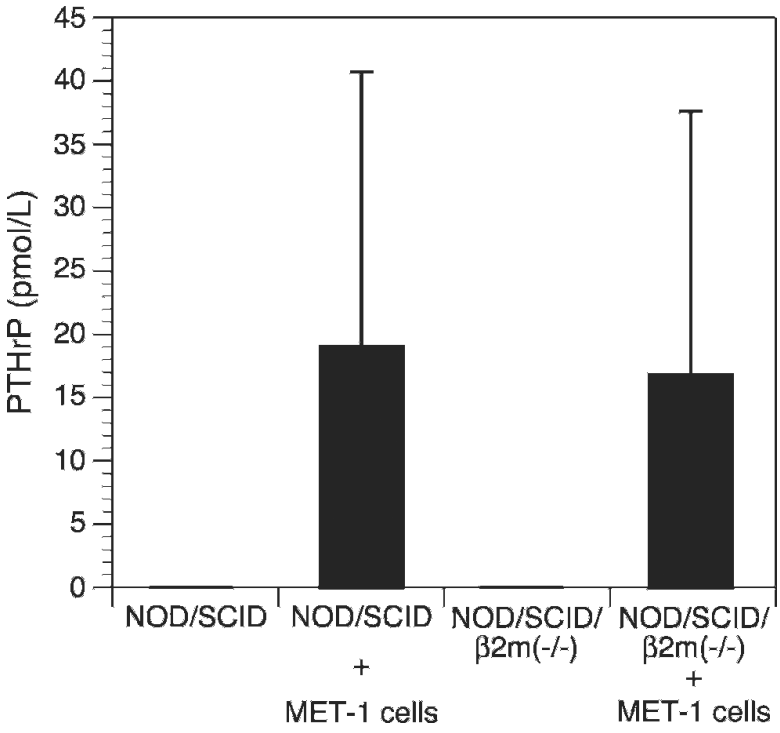

Fig. 8.

Parathyroid hormone–related protein (PTHrP) levels. PTHrP levels were increased in plasma of NOD/SCID and NOD/SCID$^{\beta 2m-/-}$ mice inoculated with MET-1 cells, whereas in the plasma of naïve animals, no PTHrP was found. The groups were the same as for calcium levels measurement.

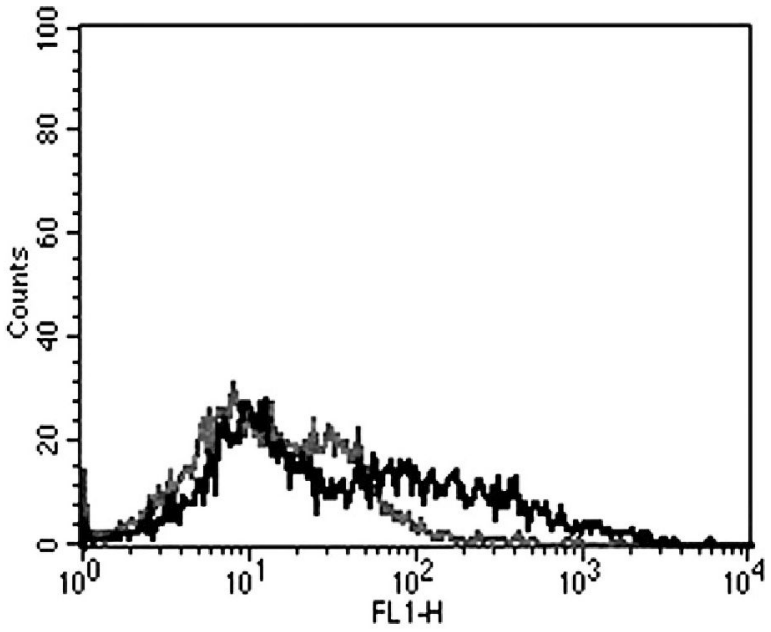

Fig. 9.

Receptor activator of nuclear factor κB ligand (RANKL) expression. Approximately 33% of the MET-1 cells were positive by flow cytometry after staining with a mouse monoclonal antibody against RANKL (grey = isotype control; black = RANKL stain). Data are representative of 3 independent experiments.

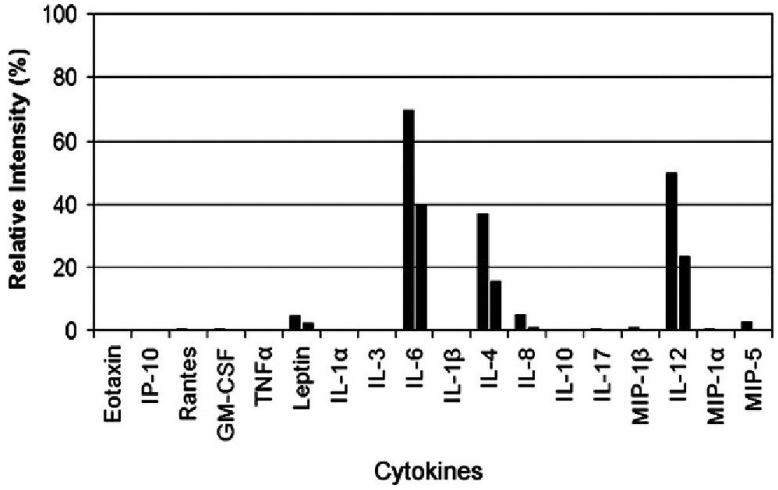

Fig. 10.

Human cytokine array. The graph shows the relative cytokine intensity for 2 groups of mice (8 animals per group) inoculated with MET-1 cells. From the 18 cytokines tested, including tumor necrosis factor-alpha, interleukin-1 (IL-1), IL-6, and macrophage inflammatory protein 1-alpha, only IL-4, IL-6, and IL-12 were markedly increased. No cytokine expression was detected on the membrane incubated with serum from naïve animals (negative control).

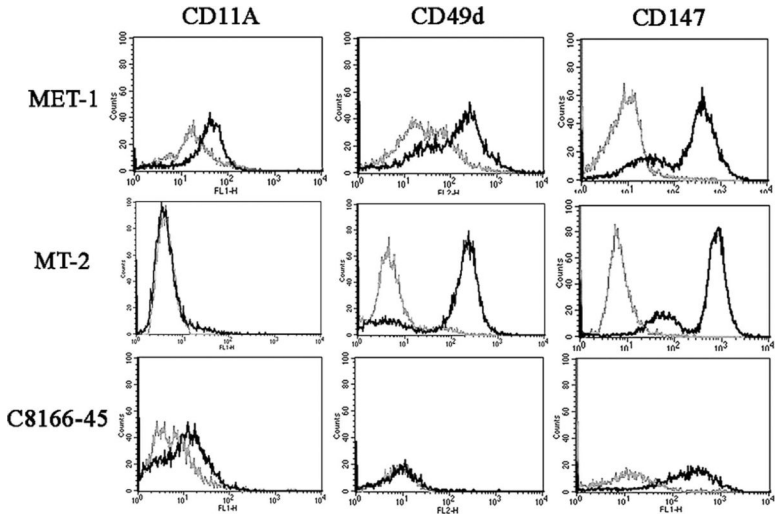

Fig. 11.

Flow cytometry for CD11a, CD49d, and CD147 (grey = isotype control, black = antibody stain). CD11a was expressed by MET-1 and C8166-45 cells but not MT-2 cells. CD49d is expressed by MET-1 and MT-2 cells but not by C8166-45 cells. CD147 is expressed by all cells. Data are representative of 3 independent experiments.

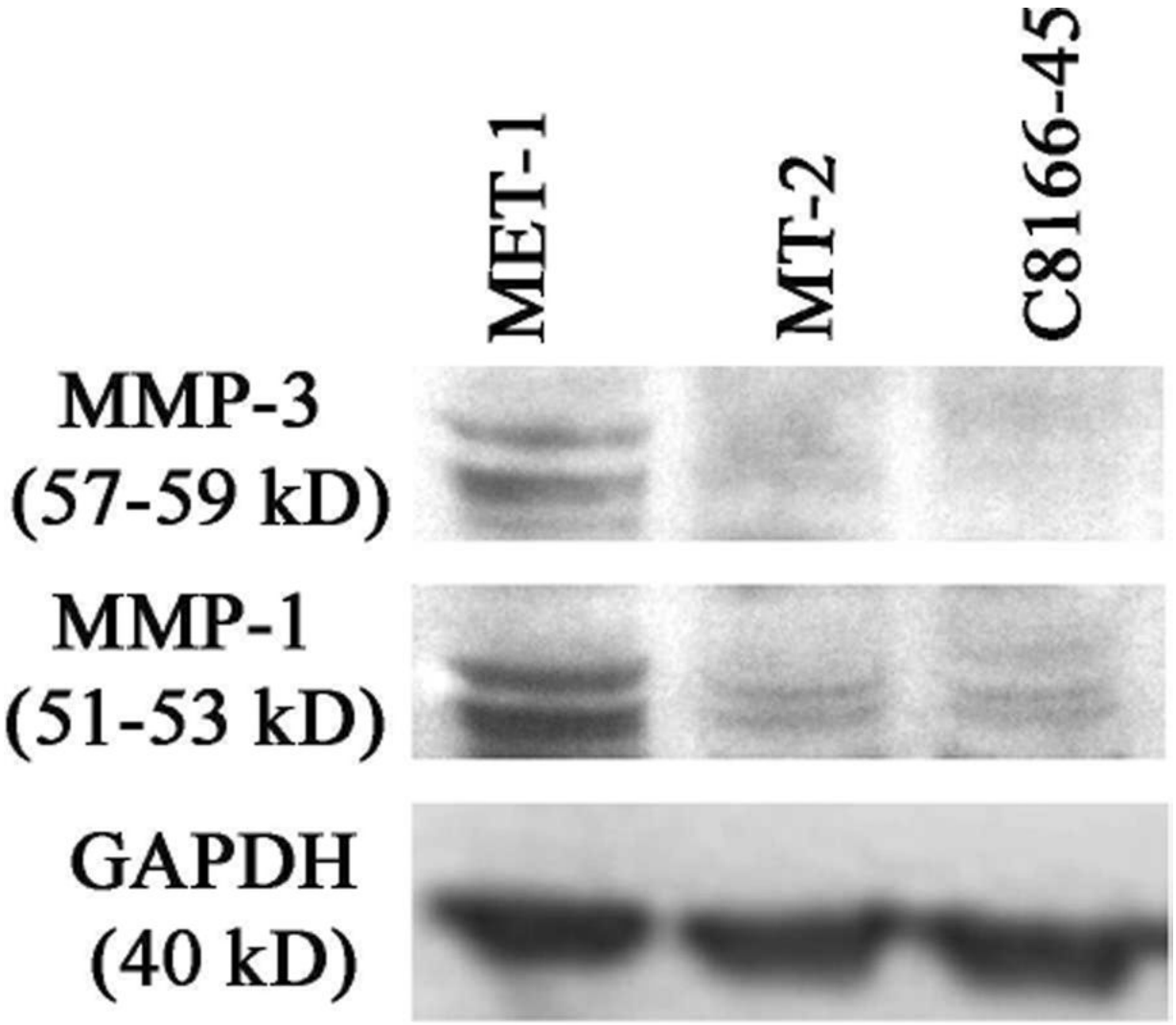

Fig. 12.
Western blot for matrix metalloproteinase 1 (MMP1) and MMP3 expression. MET-1 cells express both MMP1 and MMP3 (both MMPs seen as a double band corresponding to the proactive and active form). MMP1 was expressed weakly by MT-2 and C8166-45 cells. MMP3 was not expressed by MT-2 or C8166-45 cells. Glyceraldehyde 3-phosphate dehydrogenase was used as a loading control. Data are representative of 3 independent experiments.

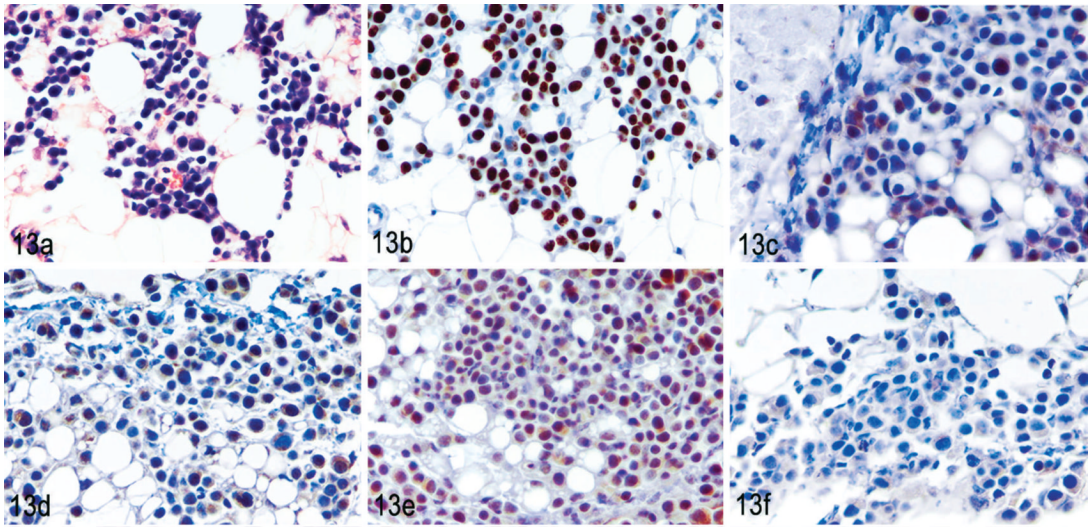

Fig. 13.

MET-1 tumors in renal fat. NOD/SCID mouse inoculated with MET-1 cells. **Fig. 13.** HE. **Fig. 13b.** MET-1 tumors stained positive with a human-specific Ki67 antibody, which proved the human origin. Immunolabeling with mAb anti-human Ki67 and hematoxylin counterstain. **Fig. 13c, d, and e.** MET-1 cells strongly expressed matrix metalloproteinase 1 (MMP1), MMP2, and MMP3, respectively, in vivo (brown staining of cytoplasm). Immunolabeling with mAb anti-MMP1, anti-MMP2, and anti-MMP3, respectively, and hematoxylin counterstain. **Fig. 13f.** MET-1 cells weakly expressed MMP9. Immunolabeling with Ab anti-MMP9 and hematoxylin counterstain.

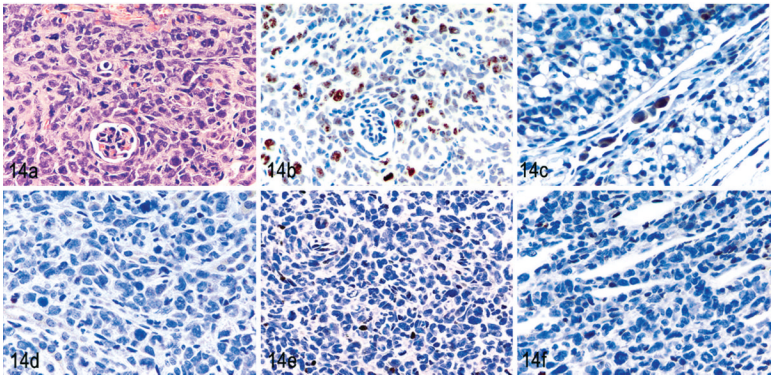

Fig. 14.

MT-2 tumors in kidney. NOD/*SCID*$^{Il2rg\ -/-}$ mouse inoculated with MT-2 cells. **Fig. 14a.** HE. **Fig. 14b.** Tumor cells stained positive with an antibody specific for human Ki67, which proved the human origin. Immunolabeling with mAb anti-human Ki67 and hematoxylin counterstain. **Fig. 14c.** A small percentage of cells weakly expressed matrix metalloproteinase 1 (MMP1). Immunolabeling with an antibody specific for MMP1 and hematoxylin counterstain. **Fig. 14d, e, and f.** MMP2, 3, and 9 are expressed weakly by rare MT-2 cells, respectively. The neutrophils that accompany MT-2 infiltration stained positively for MMPs due to residual endogenous peroxidase activity. Immunolabeling with antibodies specific for MMP2, 3, and 9, respectively, and hematoxylin counterstain.

Table 1

Mouse strains used for inoculation of adult T-cell lymphoma/leukemia cells.

	NOD/SCID	**NOD/SCID$^{\beta 2m-/-}$**	**NOD/SCID$^{IL2\text{-}R\gamma-/-}$**
Mutation/gene deletion	Catalytic subunit of the DNA-activated protein kinase (PRKDC) gene	Catalytic subunit of the DNA-activated protein kinase (PRKDC) gene	Catalytic subunit of the DNA-activated protein kinase (PRKDC) gene
		Beta-2 microglobulin gene	Gamma chain of interleukin-2 receptor gene
Deficient immune function	Lack B and T cells	Lack B and T cells	Lack B and T cells
	Reduced natural killer cell activity	Lack natural killer cell activity	Lack natural killer cell activity
			Reduced interferon gamma production

Table 2

Characterization and engraftment of cell lines infected with human T-cell leukemia virus type 1 (HTLV-1) in immune deficient mice.

Cell Line	Tax Expression	Other HTLV-I Proteins	Engraftment (no. mice engrafted/no. mice inoculated)		
			NOD/SCID	NOD/SCID$^{\beta 2m-/-}$	NOD/SCID$^{IL2\text{-}R\gamma-/-}$
MET-1	+	+	11/15 (12–14 weeks)	5/5 (9–12 weeks)	Not done
MT-2	+ +	+ +	2/5 small nodules	2/5 small nodules	5/5 (3–4 weeks)
C8166-45	+	−	0/5	0/5	0/5
ACH.2	+ +	+ +	0/5	0/5	0/5